Nanostructured Bimetallic Oxide Ion-Conducting Ceramics from Single-Source Molecular Precursors

John H. Thurston, Teyeb Ould Ely, Daniel Trahan, and Kenton H. Whitmire*

Department of Chemistry, MS-60, Rice University, 6100 Main Street, Houston, Texas 77005

Received April 21, 2003. Revised Manuscript Received September 10, 2003

A new approach for the formation of bimetallic coordination complexes of bismuth containing a 1:1 ratio of the two metal species has been developed. The strategy exploits the Lewis acidic nature of bismuth and has been used to synthesize the new complexes $BiV(O)(Hsal)(sal)(salen^*)\cdot CH_2Cl_2$ (**1**), $BiCu(Hsal)_3(salen)$ (**2**), and $BiNi(Hsal)_3(salen)\cdot CH_2Cl_2$ (**3**) (salen = ethylenebis(salicylimine), salen* = ethylenebis(3-methoxysalicylimine), sal = $O_2CC_6H_4$-2-O, Hsal = $O_2CC_6H_4$-2-OH). The compounds have been characterized spectroscopically and, in the case of **2** and **3**, by single-crystal X-ray diffraction. The decomposition of the bimetallic complexes by both thermal and hydrolytic routes has been investigated. The ability of the compounds to act as single-source precursors for the formation of bimetallic oxides has been explored. Oxide ion-conducting phases have been produced by direct pyrolysis of **1**, which results in the formation of monoclinic $BiVO_4$, and by pyrolysis of mixtures of **1** and **2** or **3**, which results in isolation of the γ'-related $Bi_2V_xM_{1-x}O_{5.5-\delta}$ (M = Cu, Ni). Thermal decomposition of the molecular compounds results in the formation of spherical oxide nanoparticles with diameters ranging from approximately 110 nm to 1 μm. Hydrolytic decomposition of the complexes results in the formation of nanoparticles with an average diameter of 40 nm. The materials produced in this manner have been characterized by scanning electron microscopy (SEM), transmission electron microscopy (TEM), and powder X-ray diffraction. Conservation of metal stoichiometry in converting the molecular precursor to the corresponding oxide has been confirmed by analysis of the materials by energy-dispersive X-ray spectroscopy.

Introduction

Oxide ion-conducting ceramics in general and bismuth vanadates ($BiVO_4$ and $Bi_2VO_{5.5}$) in particular are being examined for numerous applications including gas separation membranes,[1] oxidation catalysts,[2−4] solid-state electrolytes,[5,6] and phtotcatalysts.[7−9] Bismuth vanadates are extremely attractive materials for these applications due to their high ion conductivity,[6,10−12] thermal and electrochemical stability under repeated cycling,[13] and environmental compatibility.[14]

The physical properties of bismuth-based ceramics are critically affected by the composition and the morphology of the material and by the conditions employed in the synthesis of the binary oxide. The ion conductivity of $Bi_2VO_{5.5}$ is significantly improved by doping the material with a small amount of a late transition metal.[15] The increase in conductivity of these oxides is attributed to the stabilization of the high-temperature (γ) phase of the material by the dopant.[13] Copper and cobalt have been most heavily investigated for doping applications to produce the materials $Bi_2M_{0.1}V_{0.9}O_{5.5-\delta}$ ($BiMVO_x$). The copper-doped material is the best low-temperature oxide ion-conducting ceramic reported.[16] However, numerous other metal species have been included in the mixture to tune the reactivity of the material or to adjust the phases produced.[17,18]

The performance of bismuth vanadium oxide systems has been reported to be sensitive to the synthesis

* To whom correspondence should be addressed. E-mail: whitmir@rice.edu. Phone: 713-348-5650. Fax:713-348-5155.

(1) Steil, M. C.; Fouletier, J.; Kleitz, M.; Lagrange, G.; Del Gallo, P.; Mairesse, G.; Boivin, J. C. *BiMEVOX-based solid electrolyte inorganic membrane for separation of oxygen from air*; L'Air Liquide Societe Anonyme Pour L'Etude Et L'Exploitation Des Procedes Ge- (France), 2000.

(2) Cherrak, A.; Hubaut, R.; Barbaux, Y.; Mairesse, G. *Catal. Lett.* **1992**, *15*, 377−383.

(3) Sinhamahapatra, P. K.; Sharma, V. K.; Sinhamahapatra, S.; Bhattacharyya, S. K. *React. Kinet. Catal. Lett.* **1977**, *7*, 171−174.

(4) Sun, J.; Meng, X.; Shi, Y.; Wang, R.; Feng, S.; Jiang, D.; Xu, R.; Xiao, F. S. *J. Catal.* **2000**, *193*, 199−206.

(5) Sammes, N. M.; Tompsett, G. A.; Nafe, H.; Aldinger, F. *J. Eur. Ceram. Soc.* **1999**, *19*, 1801−1826.

(6) Wong, M. S.; Dillon, N. A.; Stranges, S. F. *Ceram. Trans.* **2000**, *109*, 11−19.

(7) Kudo, A. *J. Ceram. Soc. Jpn.* **2001**, *109*, S81−S88.

(8) Kudo, A.; Omori, K.; Kato, H. *J. Am. Chem. Soc.* **1999**, *121*, 11459−11467.

(9) Oshikiri, M.; Boero, M.; Ye, J.; Zou, Z.; Kido, G. *J. Chem. Phys.* **2002**, *117*, 7313−7318.

(10) Uma, S.; Bliesner, R.; Sleight, A. W. *Solid State Sci.* **2002**, *4*, 329−333.

(11) Hoffart, L.; Heider, U.; Huggins, R. A.; Witschel, W.; Jooss, R.; Lentz, A. *Ionics* **1996**, *2*, 34−38.

(12) Abraham, F.; Boivin, J. C.; Mairesse, G.; Nowogrocki, G. *Solid State Ionics* **1990**, *40−41*, 934−937.

(13) Pell, J. W.; Delak, K. M.; zur Loye, H. C. *Chem. Mater.* **1998**, *10*, 1764−1770.

(14) Galembeck, A.; Alves, O. L. *Thin Solid Films* **2000**, *365*, 90−93.

(15) Pell, J. W.; Delak, K. M.; zur Loye, H. C. *Mater. Res. Soc. Symp. Proc.* **1996**, *403*, 459−464.

(16) Sim, L. T.; Lee, C. K.; West, A. R. *J. Mater. Chem.* **2002**, *12*, 17−19.

(17) Thery, O.; Vannier, R. N.; Dion, C.; Abraham, F. *Solid State Ionics* **1996**, *90*, 105−110.

(18) Lee, C. K.; West, A. R. *Solid State Ionics* **1996**, *86−88*, 235−239.

10.1021/cm0342851 CCC: $25.00
Published on Web 10/22/2003

conditions.[19] Oxides produced under mild conditions, including sol−gel,[13] metal organic decompostion (MOD),[20] chemical bath deposition,[19] ionic layer deposition,[21,22] or coprecipitation techniques,[8,23] often display better properties than what is achieved from traditional solid-state syntheses. It has recently been shown that the use of molecular single-source precursors often allows for the formation of crystalline bimetallic or multimetallic oxides at conditions even milder than what can be achieved by sol−gel or coprecipitation routes.[24] This has been attributed to the intimate and controlled mixing of the metal species at the molecular level, which greatly facilitates the crystallization process of the product oxide.[25] Furthermore, these precursors can be used with both spin-casting techniques to form oxide thin films or with thermolytic or hydrolytic techniques to form discrete crystallites. Consequently, we have sought to develop a rational approach to the synthesis of bismuth vanadium oxides through the use of discrete well-defined molecular precursors. We have further sought to ensure that the synthetic approaches developed were flexible and general enough to allow for the inclusion of other transition metal species so that the effects of doping on the product oxides might be investigated directly.

We wish to report here a general synthetic approach that allows for the formation of 1:1 bimetallic complexes of bismuth by exploiting the inherent Lewis acidity of bismuth carboxylates. The new complexes BiV(O)(Hsal)-(sal)(salen*)·CH_2Cl_2 (**1**), $BiCu(Hsal)_3$(salen) (**2**), and $BiNi(Hsal)_3$(salen)·CH_2Cl_2 (**3**) (salen = ethylenebis-(salicylimine), salen* = ethylenebis(3-methoxysalicylimine), sal = $O_2CC_6H_4$-2-O, Hsal = $O_2CC_6H_4$-2-OH) have been synthesized by simple addition of the metal salen or salen* complexes to $[Bi(Hsal)_3]_n$. The bimetallic complexes have been characterized and tested for their thermolytic and hydrolytic conversion to oxide materials.

Experimental Section

All synthetic reactions were carried out using standard Schlenk or glovebox techniques under an atmosphere of purified nitrogen or argon. Solvents were purified over an appropriate reagent under argon and were distilled immediately prior to use.[26] The ligands salen and salen* were prepared by the condensation of ethylenediamine with salicylaldehyde or *o*-vanillin in toluene, by removal of the water via azeoptropic distillation.[27] Bismuth(III) salicylate, $[Bi(Hsal)_3]_n$, was prepared as previously reported.[28] To improve solubility and reactivity, the bismuth(III) salicylate was always used freshly prepared and was not isolated prior to its reaction with the transition metal complexes. Galbraith Laboratories performed all elemental analyses. TGA studies were performed on a Sieko DT/TGA 200 instrument in platinum pans under an oxygen-containing atmosphere. Approximately 5 mg of the sample to be studied was placed in a platinum pan in the furnace of a Sieko TGA/DTA instrument. The sample was heated to 600 °C at a rate of 5 °C/min in air. Phase changes in the molecular precursor that occurred during thermal decomposition were monitored by simultaneous differential thermal analysis (DTA). Powder X-ray diffraction studies were performed on a Siemens GADDS diffractometer using Cu Kα radiation (λ = 1.5418 Å). Data were collected on 2θ in the approximate range of 20°−60° as a single frame with a 1200-s exposure. Data processing of the powder diffraction results and phase identification was accomplished using the program JADE.[29] Multinuclear NMR studies of **3** were performed on a Bruker Avance instrument. The spectra were referenced to tetramethylsilane (TMS) as an internal standard. The terms sal*H* and salen*H* are employed to denote aromatic protons associated with salicylate and salen ligands, respectively. Infrared spectra of the complexes were collected on a Thermo-Nicolet 670 FT-IR using ATR methodology. UV−vis data were collected on a GBC Spectral 918 instrument as dichloromethane solutions. Mass spectra of the complexes were collected using matrix-assisted laser-desorptive ionization−time-of-flight (MALDI−TOF) techniques on a Bruker Biflex III instrument. The compound dithranol was used as a matrix in the experiments. The morphologies and relative compositions of the oxides produced through pyrolysis were examined on a FEI XL30 Schottky field-emission environmental scanning electron microscope (SEM) with an energy-dispersive X-ray spectroscopy (EDX) attachment. Transmission electron micrographs (TEM) and selected area electron diffraction data (SAED) were collected on a JEOL 2010cx instrument.

Synthesis. *Preparation of Transition Metal salen Complexes.* The transition metal salen and salen* complexes prepared in this paper were generated by the following procedure.[30,31] In a typical synthesis, a mixture of copper(II) or nickel(II) acetate or vanadyl(IV) acetylacetonate and the appropriate ligand (salen or salen*) were combined in a 1:1 ratio (5 mmol each) in 100 mL of methanol and heated until the solids completely dissolved. The reaction mixture was concentrated to 30 mL and stored for several hours at 0 °C. The product precipitated from the solution as a highly crystalline material. The solid was collected by filtration, washed with cold methanol (10 mL) and cold ether (10 mL), and dried under reduced pressure to give a free-flowing crystalline powder. Yields are better than 85%.

(1) BiV(O)(Hsal)(sal)(salen)·CH_2Cl_2 (**1**).* Compound **1** was synthesized by the addition of V(O)(salen*) (0.4 g, 1.0 mmol) to a suspension of $[Bi(Hsal)_3]_n$, prepared from the reaction of triphenylbismuth (0.4 g, 1 mmol) and salicylic acid (0.4 g, 3 mmol), in dichloromethane (20 mL). The resulting deep green solution was stirred at room temperature for 24 h. During this time an emerald green powder was deposited. The solid was collected by filtration, washed with dichloromethane and diethyl ether, and dried briefly under reduced pressure. Careful recrystallization of the complex resulted in the formation of green needles. Repeated attempts to grow crystals of **1** suitable for single-crystal X-ray diffraction experiments have not yet been successful. Compound **1**: yield, 0.72 g (0.78 mmol, 88%). Elemental analysis: % observed (% calculated for $C_{33}H_{29}BiCl_2N_2O_{11}V$): C, 41.61 (41.27); H, 3.17 (3.04); N, 3.08 (2.92). IR: 1618, 1601, 1554, 1480, 1467, 1446, 1395, 1368, 1309, 1280, 1242, 1221, 1163, 1140, 1078, 972, 869, 819, 771, 757,

(19) Neves, M. C.; Trindade, T. *Thin Solid Films* **2002**, *406*, 93−97.
(20) Galembeck, A.; Alves, O. L. *J. Mater. Sci.* **2002**, *37*, 1923−1927.
(21) Tolstoy, V. P.; Tolstobrov, E. V. *Solid State Ionics* **2002**, *151*, 165−169.
(22) Hirota, K.; Komatsu, G.; Takemura, H.; Yamaguchi, O. *Ceram. Int.* **1992**, *18*, 285−287.
(23) Tokunaga, S.; Kato, H.; Kudo, A. *Chem. Mater.* **2001**, *13*, 4624−4628.
(24) Hubert-Pfaltzgraf, L. G. *Inorg. Chem. Commun.* **2003**, *6*, 102−120.
(25) Pandey, A.; Gupta, V. D.; Noth, H. *Eur. J. Inorg. Chem.* **1999**, 1291.
(26) Armarego, W. L. F.; Perry, D. D. *Purification of Laboratory Chemicals*, 4th ed.; Butterworth-Heinemann: Boston, 1996.
(27) Smith, M. B.; March, J. *March's Advanced Organic Chemistry: Reactions, Mechanisms, and Structure, 5th Edition*; Wiley: New York, 2001.
(28) Thurston, J. H.; Whitmire, K. H. *Inorg. Chem.* **2002**, *41*, 4194−4205.
(29) MDI, *JADE, XRD Pattern-Processing for the PC* 2.1; Livermore, CA, 1994.
(30) Riley, P. E.; Pecoraco, V. L.; Carrano, C. J.; Bonadies, J. A. *Inorg. Chem.* **1986**, *25*, 154−160.
(31) Cashin, B.; Cunningham, D.; Daly, P.; McArdle, P.; Munroe, M.; Chonchubhair, N. N. *Inorg. Chem.* **2002**, *41*, 773−782.

737, 705, 667. MALDI−TOF MS: 741 (40%, **1**-H_2sal), 605 (25%, **1**-2H_2sal), 395 (100%, V(O)(salen*)). mp: 220−224°C (dec). ϵ_o = 3900 L·mol^{-1}·cm^{-1}.

*(2) BiCu(Hsal)$_3$(salen) (**2**).* To a suspension of [Bi(Hsal)$_3$]$_n$, prepared from the reaction of triphenylbismuth (0.4 g, 1 mmol) and salicylic acid (0.4 g, 3 mmol) in dichloromethane, was added Cu(salen) (0.3 g, 1.0 mmol) in 10 mL of dichloromethane. The resulting deep burgundy solution was stirred at room temperature for 10 min to complete dissolution of the bismuth and then allowed to stand undisturbed for 24 h at room temperature. During this time large crimson crystals deposited in the reaction flask. The solid was collected by filtration, washed with dichloromethane and diethyl ether, and dried briefly under reduced pressure. Compound **2**: yield, 0.76 g (0.89 mmol, 86%). Elemental analysis: % observed (% calculated for $C_{37}H_{29}N_2O_{11}BiCu$): C, 46.68 (46.77); H, 3.15 (3.08); N, 2.90 (2.95). FT-IR: 1623, 1600, 1591, 1540, 1525, 1469, 1441, 1375, 1335, 1284, 1251, 1196, 1155, 1083, 1033, 903, 870, 851, 821, 787, 767, 752, 699, 667. MALDI−TOF MS: 812 (22%, **2**-H_2sal), 676 (48%, **2**-2H_2sal), 539 (35%, **2**-3H_2sal), 353 (100%, Cu(salen)). mp: 220−222 °C. ϵ_o = 12211 L·mol^{-1}·cm^{-1}.

*(3) BiNi(Hsal)$_3$(salen)·CH_2Cl_2 (**3**).* Compound **3** was prepared in a manner analogous to **2** with the substitution of Ni(salen) for Cu(salen) and was isolated as bright orange crystals. Yield: 0.78 g (0.87 mmol, 85% yield). ^{1}H NMR ($CDCl_3$, 500 MHz, 25 °C): 3.41 (s, −CH_2, 4H), 6.54 (t, salen*H*, 2H, J = 7.02 Hz), 6.90 (t, sal*H*, 3H, J = 7.59 Hz), 6.97 (d, sal*H*, 3H, J = 8.35 Hz), 7.01 (d, salen*H*, 2H, J = 7.86 Hz), 7.05 (d, salen*H*, 2H, J = 8.43 Hz), 7.21 (td, salen*H*, 2H, J^1 = 8.57 Hz, J^2 = 1.69 Hz), 7.43 (s, salen*H*, 2H), 7.47 (t, sal*H*, 3H, J = 8.66 Hz), 8.11 (d, sal*H*, 3H, J = 7.81 Hz), 10.71 (s, OH, 3H). ^{13}C{^{1}H} NMR ($CDCl_3$, 125 MHz, 25 °C): 58.65, 111.68, 115.48, 117.90, 119.58, 120.15, 121.97, 130.96, 132.38, 134.32, 136.73, 162.12, 162.41, 172.74. Elemental analysis: % observed (% calculated for $C_{37}H_{31}N_2O_{12}BiNi$): C, 46.42 (46.13); H, 3.06 (3.24); N, 2.91 (2.97). IR: 1624, 1589, 1547, 1478, 1447, 1393, 1347, 1289, 1246, 1221, 1154, 1091, 1063, 1027, 960, 904, 873, 820, 757, 701, 667. MALDI−TOF MS: 825 (32%, **3**-H_2sal), 671 (54%, **3**-2H_2sal-H_2O), 533 (25%, **3**-3H_2sal-H_2O), 325 (100%, Ni-(salen)). mp: 280 °C (dec). ϵ_o = 6485 L·mol^{-1}·cm^{-1}.

Thermal Synthesis of Oxide Samples. Oxide samples of **1** were prepared by annealing samples of the molecular complex for 2 h at 750 °C in air. The resulting materials were cooled to room temperature and analyzed by SEM or ground to a fine powder using an agate mortar and pestle and analyzed by powder X-ray diffraction and EDX. Samples of **2** and **3** were treated similarly but were annealed at 450 °C in air for 2 h.

Termetallic samples were synthesized by a general procedure listed here. The desired amounts of the two molecular precursors were dissolved in dichloromethane. These solutions were mixed and stirred for 5 min, and then the solvent was removed under reduced pressure. The resulting solid was dried for an additional 30 min under vacuum. Pyrolysis of this mixture for 2 h at 750 °C in air resulted in the formation of the desired termetallic phases.

Hydrolytic Synthesis of Oxide Samples. Nanoscale particles were prepared using a modification of the method reported by O'Brien and co-workers,[32] and a general procedure is presented here. A sample of the molecular precursor **1** (0.355 g, 0.5 mmol) and stearic acid (0.428 g, 1.5 mmol) was placed in 50 mL of diphenyl ether under argon. The green solution was heated to 150 °C and a 30% solution of hydrogen peroxide (0.2 mL) was introduced by syringe with stirring. The solution became turbid and the color changed from green to brown. These reaction conditions were maintained for 36 h. The product was collected by centrifugation and washed with diethyl ether (2 × 15 mL) and with dichloromethane (1 × 15 mL) until the washings were no longer colored. The particles were dispersed in absolute ethanol by sonication to form an orange-red suspension that was used for electron microscopy experiments.

Solid State Structures. Compounds **2** and **3** were studied on a Bruker Smart 1000 diffractometer equipped with a CCD area detector. The data were corrected for Lorentz and polarization effects. Absorption correction was applied using the program SADABS.[33] No appreciable decay of the crystals was detected during data collection. Heavy atoms in the compounds were located using Patterson methods with the SHELXTL software package.[34] All other atoms were located by successive Fourier difference maps and were refined using the full-matrix least-squares technique on F^2. All non-hydrogen atoms, with the exceptions discussed below, were refined anisotropically. Hydrogen atoms in all of the complexes were placed in calculated positions and allowed to ride on the adjacent atom. Hydrogen atoms associated with phenolic oxygen atoms were placed in calculated positions and refined geometrically using a riding model. The hydrogen atom was oriented so that the most likely hydrogen bond—in this case to a carboxylate oxygen of the same molecule—was realized. Investigation of the packing structures of the molecules using the program PLATON did not reveal the presence of intermolecular hydrogen bonds.[35] Refinement of the model parameters against the observed data led to convergence. Compound **2**: One of the salicylate ligands was found to have a hydroxyl group disordered over two positions in the crystal lattice. This disorder was modeled with each potential hydroxyl group location receiving partial occupancy. The refined relative populations for the two hydroxyl group positions were 0.6 and 0.4. The carbon atoms of the disordered ligand were refined isotropically. Compound **3**: One of the salicylate ligands was disordered with the phenyl ring occupying two positions in the crystal lattice. The two phenyl ring positions of this salicylate ligand were refined as rigid bodies. The disorder in the molecule was treated similarly to **2**, with the refined relative populations for the two positions of the disordered ligand being 0.4 and 0.6.

Results and Discussion

Soft chemical approaches have been used to generate both bimetallic oxides and metastable oxide phases at conditions significantly milder than what is required by traditional solid-state syntheses.[36] Specifically, molecular single-source precursors are able to produce multimetallic oxides under comparatively mild conditions[24,37] and in very high purity due to the intimate mixing of the metal species at the molecular level.[38] The presence of bridging or chelating organic ligands in these molecular precursors successfully arrests unwanted metal segregation during oxide formation[39,40] and allows for decomposition and crystallization processes to occur at conditions significantly milder than what is required for traditional solid-state syntheses.[32,40] The mild conditions under which the product oxides are produced presents the possibility of improving the reactivity of the systems by controlling the morphology, particle sizes, and phases present. These approaches have recently been shown to produce crystalline samples of bimetallic bismuth oxides containing titanium, nio-

(32) O'Brien, S.; Brus, L.; Murray, C. B. *J. Am. Chem. Soc.* **2001**, *123*, 12085−12086.

(33) Sheldrick, G. *SADABS* 5.1; University of Göttingen: Göttingen, 1997.

(34) Sheldrick, G. *SHELXTL* 6.1; University of Göttingen: Göttingen, 2001.

(35) Spek, A. L. *Platon, A Multipurpose Crystallographic Tool*; Utrecht University: Utrecht, The Netherlands, 2001.

(36) Gopalakrishnan, J. *Chem. Mater.* **1995**, *7*, 1265−75.

(37) Hubert-Pfaltzgraf, L. G. *New J. Chem.* **1995**, *19*, 727−750.

(38) Gleizes, A.; Julve, M.; Kuzmina, A.; Alikhanyan, A.; Lloret, F.; Malkerova, I.; Sanz, J. L. *Eur. J. Inorg. Chem.* **1998**, *1998*, 1169−1174.

(39) Boulmaaz, S.; Papiernik, R.; Hubert-Pfaltzgraf, L. G.; Spete, B.; Vaissermann, J. *J. Mater. Chem.* **1997**, *7*, 2053−2061.

(40) Thurston, J. H.; Whitmire, K. H. *Inorg. Chem.* **2003**, ASAP article.

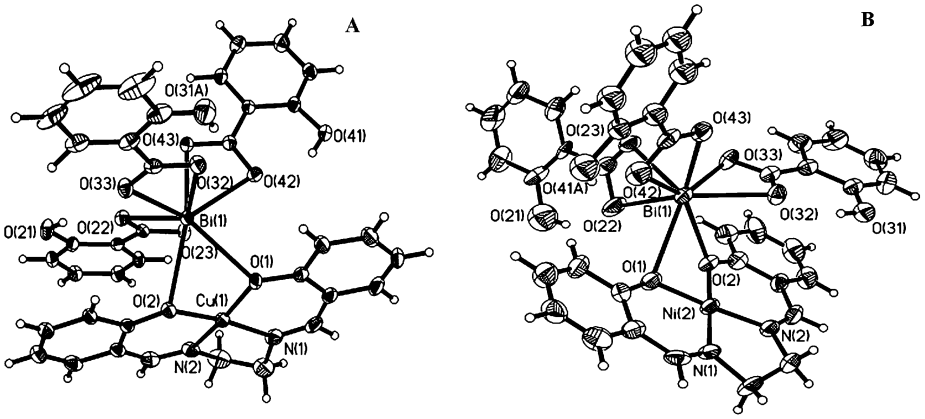

Figure 1. ORTEP representation of **2** (A) and **3** (B). Thermal ellipsoids are drawn at the 30% probability level. For clarity, only one orientation of the disordered salicylate ligand has been shown in each case, and the lattice solvent in $BiNi(Hsal)_3(salen)$ has been omitted.

bium, or tantalum.[28,40] Consequently, we have sought to develop a rational approach to the synthesis of bismuth-based oxide ion-conducting ceramics through the use of well-defined molecular precursors.

The ability of transition metal salen complexes to coordinate to transition[41,42] and lanthanide metal salts[43,44] as well as main-group organometallic complexes[31] has been well-documented. There is marked similarity between the chemistry of the lanthanides and that of bismuth. For example, both lanthanum and bismuth react to form nona-aqua complexes $M^{III}(H_2O)_9(OTf)_3$ (M^{III} = La, Bi; OTf = O_3SCF_3). Single crystal X-ray diffraction studies of these salts have shown that they are isomorphous. Accordingly, we have found that bismuth(III) salicylate reacts smoothly with transition metal salen complexes to produce well-defined bimetallic systems. The steric bulk of the salen complex restricts the number of transition metal complexes that can be accommodated into bismuth's coordination sphere and allows for the formation of 1:1 adducts exclusively.

Complexes **2** and **3** have been characterized by single-crystal X-ray diffraction (Figure 1). Repeated attempts to grow single crystals of **1** suitable for single-crystal X-ray diffraction have not yet been successful. Pertinent details of the diffraction experiments are provided in Tables 1−3. The complexes are essentially isostructural in the solid state. Complex **3** cocrystallizes with a single molecule of dichloromethane in the crystal lattice. The solvent can be removed from the product by placing the sample under reduced pressure for 24 h. In both cases, the bismuth center is formally eight-coordinate and has approximately a capped pentagonal bipyramidal geometry, while the transition metals are four-coordinate and square planar. The salicylate ligands interact with the bismuth center through both oxygen atoms of the carboxylate ligand, although the bond distances of two oxygen atoms to the metal center are slightly asymmetric. The interaction of the salen complex with the bismuth center occurs through bridging interactions of the phenolic oxygen atoms. The $Bi-O_{salicylate}$ bond distances range from 2.338(4) to 2.529(4) Å in **2** and from 2.311(9) to 2.548(8) Å in **3**. The $Bi-O_{salen}$ bond distances are 2.709(4) and 2.729(4) Å in **2** and 2.639(8) and 2.743(8) Å in **3**. The angle between the plane defined by the bismuth atom and the two phenolic

Table 1. Crystallographic Data for New Compounds

formula	$C_{37}H_{29}N_2O_{11}BiCu$	$C_{37}H_{29}N_2O_{11}BiNi$
fw	951.15	1030.24
space group	$P\bar{1}$	$P2_1/n$
Z	2	4
crystal system	triclinic	monoclinic
A (Å)	10.240(2)	10.663(2)
B (Å)	13.279(3)	19.361(4)
C (Å)	13.705(3)	19.245(4)
α (deg)	93.17(3)	
β (deg)	108.60(3)	103.50(3)
γ (deg)	106.38(3)	
V, Å^3	1672.7(6)	3863.5(13)
D(calc), g/mm	1.889	1.771
temp (°C)	25	25
λ, Mo Kα (Å)	0.71073	0.71073
μ (cm^{-1})	59.59	52.37
R1[a]	0.0282	0.0581
WR2[b]	0.0343	0.0960

[a] Conventional *R* on F_{hkl}: $[\sum|F_o| - |F_c|]/\sum|F_o|$. [b] Weighted *R* on $|F_{hkl}|^2$: $\{\sum[w(F_o^2 - F_c^2)^2]/\sum[w(F_o^2)^2]\}^{1/2}$.

Table 2. Bond Lengths (Å) and Angles (deg) for 2

Bi(1)−O(43)	2.305(4)	Bi(1)−O(1)	2.709(4)
Bi(1)−O(22)	2.338(4)	Bi(1)−O(2)	2.729(4)
Bi(1)−O(33)	2.376(4)	Cu(1)−O(1)	1.905(4)
Bi(1)−O(42)	2.439(4)	Cu(1)−O(2)	1.912(4)
Bi(1)−O(23)	2.471(3)	Cu(1)−N(1)	1.932(5)
Bi(1)−O(32)	2.529(4)	Cu(1)−N(2)	1.933(5)
O(43)−Bi(1)−O(22)	76.95(13)	O(42)−Bi(1)−O(1)	72.88(12)
O(43)−Bi(1)−O(33)	85.07(13)	O(23)−Bi(1)−O(1)	77.81(12)
O(22)−Bi(1)−O(33)	75.11(12)	O(32)−Bi(1)−O(1)	113.10(12)
O(43)−Bi(1)−O(42)	54.99(13)	O(43)−Bi(1)−O(2)	144.59(12)
O(22)−Bi(1)−O(42)	121.35(12)	O(22)−Bi(1)−O(2)	74.81(12)
O(33)−Bi(1)−O(42)	124.92(13)	O(33)−Bi(1)−O(2)	107.53(12)
O(43)−Bi(1)−O(23)	76.55(12)	O(42)−Bi(1)−O(2)	127.19(11)
O(22)−Bi(1)−O(23)	54.10(11)	O(23)−Bi(1)−O(2)	69.72(11)
O(33)−Bi(1)−O(23)	128.50(13)	O(32)−Bi(1)−O(2)	136.01(11)
O(42)−Bi(1)−O(23)	81.40(12)	O(1)−Bi(1)−O(2)	58.66(11)
O(43)−Bi(1)−O(32)	78.23(13)	O(1)−Cu(1)−O(2)	88.49(15)
O(22)−Bi(1)−O(32)	124.05(12)	O(1)−Cu(1)−N(1)	94.00(19)
O(33)−Bi(1)−O(32)	53.42(13)	O(2)−Cu(1)−N(1)	172.77(18)
O(42)−Bi(1)−O(32)	80.05(12)	O(1)−Cu(1)−N(2)	171.42(18)
O(23)−Bi(1)−O(32)	154.27(13)	O(2)−Cu(1)−N(2)	93.74(18)
O(43)−Bi(1)−O(1)	124.31(12)	Cu(1)−O(1)−Bi(1)	97.13(14)
O(22)−Bi(1)−O(1)	122.38(11)	Cu(1)−O(2)−Bi(1)	96.28(13)
O(33)−Bi(1)−O(1)	146.95(12)		

(41) O'Connor, C. J.; Freyberg, D. P.; Sinn, E. *Inorg. Chem.* **1979**, *18*, 1077−1088.
(42) Sunatsuki, Y.; Matsuo, T.; Nakamura, M.; Kai, F.; Matsumoto, N.; Tuchagues, J.-P. *Bull. Chem. Soc. Jpn.* **1998**, *71*, 2611.
(43) Kido, T.; Ikuta, Y.; Sunatsuki, Y.; Ogawa, Y.; Matsumoto, N.; Re, N. *Inorg. Chem.* **2002**, *42*, 398−408.
(44) Kido, T.; Nagasato, S.; Sunatsuki, Y.; Matsumoto, N. *J. Chem. Soc., Chem. Commun.* **2000**, *21*, 2113-2114.

Table 3. Bond Lengths (Å) and Angles (deg) for 3

Bi(1)−O(33)	2.293(9)	Bi(1)−O(2)	2.639(8)
Bi(1)−O(23)	2.311(9)	Bi(1)−O(1)	2.743(8)
Bi(1)−O(43)	2.348(8)	O(1)−Ni(2)	1.845(9)
Bi(1)−O(22)	2.515(10)	N(1)−Ni(2)	1.813(11)
Bi(1)−O(42)	2.529(10)	Ni(2)−N(2)	1.845(11)
Bi(1)−O(32)	2.548(8)	Ni(2)−O(2)	1.865(8)
O(33)−Bi(1)−O(23)	77.9(3)	O(22)−Bi(1)−O(2)	76.4(3)
O(33)−Bi(1)−O(43)	82.9(3)	O(42)−Bi(1)−O(2)	141.3(3)
O(23)−Bi(1)−O(43)	76.6(3)	O(32)−Bi(1)−O(2)	72.8(3)
O(33)−Bi(1)−O(22)	94.6(4)	O(33)−Bi(1)−O(1)	138.6(3)
O(23)−Bi(1)−O(22)	52.6(3)	O(23)−Bi(1)−O(1)	119.9(3)
O(43)−Bi(1)−O(22)	128.2(3)	O(43)−Bi(1)−O(1)	135.2(3)
O(33)−Bi(1)−O(42)	134.6(3)	O(22)−Bi(1)−O(1)	74.5(3)
O(23)−Bi(1)−O(42)	79.6(3)	O(42)−Bi(1)−O(1)	86.7(3)
O(43)−Bi(1)−O(42)	53.6(3)	O(32)−Bi(1)−O(1)	110.0(3)
O(22)−Bi(1)−O(42)	102.2(4)	O(2)−Bi(1)−O(1)	55.3(3)
O(33)−Bi(1)−O(32)	52.5(3)	Ni(2)−O(1)−Bi(1)	95.0(3)
O(23)−Bi(1)−O(32)	127.2(3)	N(1)−Ni(2)−N(2)	85.8(5)
O(43)−Bi(1)−O(32)	80.2(3)	N(1)−Ni(2)−O(1)	94.8(5)
O(22)−Bi(1)−O(32)	136.7(3)	N(2)−Ni(2)−O(1)	175.6(4)
O(42)−Bi(1)−O(32)	120.9(3)	N(1)−Ni(2)−O(2)	178.5(4)
O(33)−Bi(1)−O(2)	83.5(3)	N(2)−Ni(2)−O(2)	94.8(5)
O(23)−Bi(1)−O(2)	123.1(3)	O(1)−Ni(2)−O(2)	84.6(4)
O(43)−Bi(1)−O(2)	152.7(3)	Ni(2)−O(2)−Bi(1)	98.0(3)

oxygen atoms and the plane defined by the transition metal salen complex is ca. 42.8° in **2** and is ca. 49.5° in **3**, illustrating that the bismuth atom sits above the salen ligand.

The salicylate ligands in compound **2** are arranged so that the angle between the planes defined by two of the ligands is ca. 26.9° while the third ligand forms angles of ca. 78.5° and 103.5° with the first two. Two of the salicylate ligands are oriented so that they are essentially parallel with one another, while the third is perpendicular to these two. The parallel ligands are also parallel to the plane of the salen ligand, and there is a short π-stacking contact between one of the salicylate ligands of compound **2** and the salen ligand of an adjacent molecule ($d_{\text{centroid−centroid}}$ = 4.648(6) Å). This interaction may play a significant role in stabilizing the crystal lattice. In contrast, the angles between the planes defined by the salicylate ligands of compound **3** are ca. 108.6°, 95.6°, and 95.1°. These angles illustrate that all of the salicylate ligands in **3** are oriented approximately perpendicular to one another and, consequently, only one of the salicylate ligands is parallel to the plane of the transition metal salen group. Compound **3** demonstrates short nonbonding metal−metal interactions between nickel atoms ($d_{\text{Ni−Ni}}$ = 3.357(3) Å) on adjacent molecules. The intermolecular contacts observed for **2** and **3** are similar to what has been reported for lanthanide complexes of copper and nickel salen compounds.[38] The C_{ipso}−Bi−C_{ipso} angles in **2** and **3** range from 88.93(15)° to 127.15(17)° and from 96.9(4)° to 125.1(3)°, respectively, and compare well with what has been reported for the structurally similar complex [Bi(C_6H_4-2-OMe)$_3$(μ-O)]$_2$.[45]

Unlike **2** and **3**, direct reaction of bismuth salicylate with V(O)salen produced compounds that were so labile that the isolation of the pure bimetallic complex was not achieved. The stability of the vanadium complexes was greatly improved by replacing the salen ligand with salen*. The methoxy groups on the salen* ligand have been previously observed to improve the ability of the compound to complex with Lewis acidic centers.[31] In this case, the bimetallic coordination complex **1** is readily isolated and purified. However, the greater steric constraints of the salen* ligand apparently result in elimination of a molecule of salicylic acid from the bismuth complex to give Bi(Hsal)(sal)·V(O)(salen*), rather than Bi(Hsal)$_3$·V(O)(salen*), as indicated by elemental analysis and mass spectrometry. This analysis is described in further detail below.

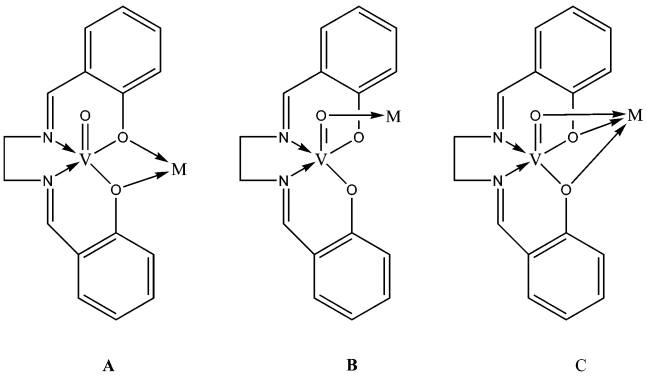

Figure 2. Potential modes of interaction of vanadyl(IV) salen with a Lewis acidic metal center (M).

The bimetallic nature of the compounds presented here is retained in the gas phase as confirmed by mass spectrometry. In all cases, the highest ion that was detected corresponded to the bimetallic complex minus a salicylate ligand (Hsal). The identity of these complexes has been confirmed by matching the isotopic distribution of the peaks to theoretical distribution predicted for the bimetallic complexes. In the case of complexes **2** and **3**, this corresponds to the Bi(Hsal)$_2$M(salen)]$^+$ (M = Cu, Ni) fragment; however, in the case of **1**, the largest ion observed corresponds to Bi(sal)V(O)(salen*)]$^+$. These results are consistent with compounds **2** and **3** containing three salicylate ligands at the bismuth center, while complex **1** contains only two. In the latter case, charge balance requires that one of the remaining salicylate ligands be doubly deprotonated. This difference in reactivity of the salen and the salen* complexes has precedent in the reaction of Bi(Hsal)$_3$ with 2,2′-bipyridine and 1,10-phenanthroline. The former ligand yields the adduct [Bi(Hsal)$_3$(bipy)·(C_7H_8)]$_2$, while the latter undergoes H_2sal elimination and produces the complex [Bi(Hsal)(sal)(phen)·(C_7H_8)]$_2$.[46] Elemental analyses of the three compounds support these formulations.

There are several possible modes of interaction between the bismuth center and the vanadyl complex that are not possible with the simple M(salen) compounds (Figure 2). The vanadium can coordinate to the bismuth via the phenolic oxygen atoms of the salen ligand as observed in complexes **2** and **3** (Figure 2A), but it can also coordinate to the bismuth atom through the vanadyl oxygen (Figure 2B) or, potentially, through both the vanadyl oxygen and the phenolic oxygen atoms (Figure 2C).

Only the coordination modes represented in Figure 4A,B have been observed for vanadium complexes of the main group elements.[31,47,48] Infrared spectroscopy has been used to elucidate the probable structure of com-

(45) Matano, Y.; Nomura, H. *J. Am. Chem. Soc.* **2001**, *123*, 6443−6444.

(46) Thurston, J. H.; Marlier, E. E.; Whitmire, K. H. *J. Chem. Soc., Chem. Commun.* **2002**, *23*, 2834−2835.

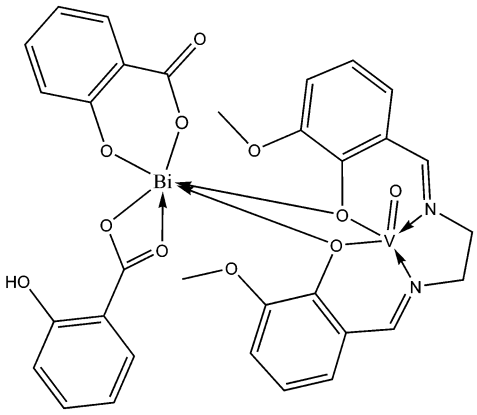

Figure 3. Proposed structure of **1**.

pound **1** in the solid state by examining the V═O vibration frequency before and after reaction of the salen* complex with bismuth salicylate. Theoretical and experimental studies have established that the vanadyl oxygen bond possesses significant triple-bond character.[49] Coordination of a Lewis acid to the vanadyl oxygen atom results in reduction of the bond order to 2 and a subsequent shift of the vibration to lower frequency.[31] This has been demonstrated in the complex $V(OBPh_3)(C_{22}H_{22}N_4)$, in which the V═O peak is reported to shift from 965 to 919 cm^{-1}.[50] In contrast, coordination of a main group element to the phenolic oxygen atom has only been shown to reduce electron density at the metal center, increasing the bond order of the vanadyl oxygen and shifting the observed peak to higher frequency.[31] Infrared analysis of complex **1** reveals that the V═O peak shifts from 969 cm^{-1} for the uncomplexed ligand to the higher frequency of 990 cm^{-1} for the bimetallic coordination compound. These results are consistent with observations for the coordination of the transition metal complex to the bismuth center via the phenolic oxygen atoms and fit with the reactivity that has been established for this system by compounds **2** and **3** (Figure 3).

Thermal and Hydrolytic Studies

The thermal decomposition of compounds **1**−**3** has been examined by TGA/DTA.

Compound **1** begins to decompose at 200 °C and the final oxide is obtained at 430 °C. The thermal decomposition of the complexes was found to proceed under mild conditions, with the decomposition of the complex **1** complete at almost 70 °C less than what has been reported for similar systems.[20] The decomposition of **1** occurs in several steps, and simultaneous differential thermal analysis of the material revealed the presence of two strong exotherms at 368 and 410 °C. The final event corresponds to a reorganization of the oxide lattice, as essentially no mass is lost in that process. The exact cause of the exothermic event at 368 °C is not clear, but it may relate to a conversion of the V^{IV} species present in the molecular precursor to the V^{V} ions that are present in the final oxide.

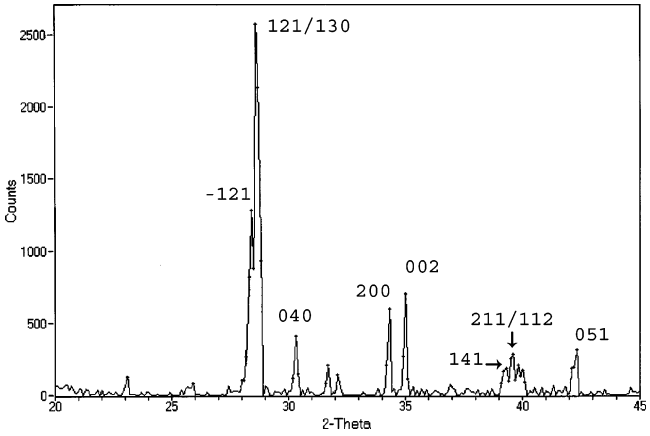

Figure 4. Indexed powder X-ray diffraction data of the material produced from the thermal decomposition of **1**. All of the peaks are indexed to the monoclinic form of $BiVO_4$.

The product produced via the pyrolysis of **1** has been explored by powder X-ray diffraction and by scanning electron microscopy. Powder X-ray diffraction studies demonstrated that heating a sample of **1** for 2 h at 450 °C produces monoclinic $BiVO_4$ as the only crystalline phase (Figure 4). This stoichiometry of the oxide agrees with what is present in the molecular precursor and indicates that metal segregation does not occur during the pyrolysis event. Investigation of the oxides by SEM illustrates that the material produced in this manner is composed of highly aggregated oxide spheres (Figure 5A). The isolation of discrete dispersable oxide spheres of $BiVO_4$ by direct thermolysis of **1** has not been achieved. Increasing the annealing conditions of the material to 24 h at 750 °C did not result in any change in the phases present in the sample. However, the average diameter of the particles present in the sample was found to increase from 110 nm to approximately 65 μm (Figure 5B). In this case, the morphology of the sample has come to resemble that which is commonly associated with the monoclinic phase of $BiVO_4$.

Similar experiments have been performed on compounds **2** and **3**, due not only to the fact that the doped samples of bismuth vanadate have been shown to be extremely efficient oxide ion conductors but also to the fact that the binary oxides produced from these mixtures are potentially useful as well. For example, bismuth−nickel oxides are being explored as catalysts for the dehydrogenation of hydrocarbons[51] and for the transalkylation of aromatic hydrocarbon systems.[52] Similarly, bismuth−copper oxides have been investigated as catalysts for the synthesis of 1,4-butynediol from acetylene and formaldehyde[53] and for the removal of nitrogen oxides from exhaust streams.[54] However, the

(47) Choudhary, N. F.; Hitchcock, P. B.; Leigh, G. J.; Ng, S. W. *Inorg. Chim. Acta* **1999**, *293*, 147−154.
(48) Cashin, B.; Cunningham, D.; Gallagher, J. F.; McArdle, P.; Higgins, T. *J. Chem. Soc., Chem. Commun.* **1989**, *19*, 1445−1446.
(49) Di Bella, S.; Lanza, G.; Gulino, A.; Fragalà, I. *Inorg. Chem.* **1996**, *35*, 3885−3890.
(50) Yang, C.-H.; Ladd, J. A.; Goedken, V. L. *J. Coord. Chem.* **1988**, *18*, 317−34.
(51) Al-Zahrani, S. M.; Abasaeed, A. E.; Elbashir, N. O.; Abdulwahed, M. A. *New catalyst systems for the oxidative dehydrogenation of hydrocarbons*; Saudi Basic Industries Corporation: Saudi Arabia, 2001.
(52) Chen, Q.; Xie, Z.; Bao, J. *Catalyst for disproportionation and transalkylation of toluene and C9 aromatic hydrocarbon*; Shanghai Institute of Petrochemical Research: China, 2000.
(53) Zhang, W.; Wang, R.; Liang, Y. *Regeneration of catalysts for synthesizing 1,4-butynediol from formaldehyde and acetylene by a slurry-bed reaction*; Beijing Chemical Institute: China, 1996.
(54) White, J. H. *Catalyst for removing nitrogen oxides from exhaust streams in absence of reducing agents*; Electric Power Research Institute: USA, 1999.

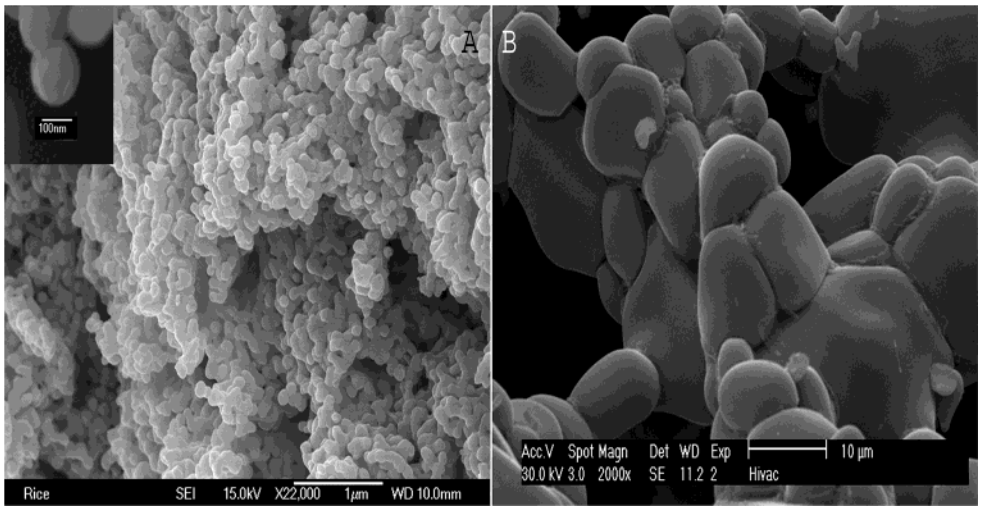

Figure 5. SEM image of the pyrolysis product of **1** produced after heating the molecular precursor for 15 min at 450 °C (A) and for 2 h at 750 °C (B). The inset figure details a single bimetallic oxide sphere, with a diameter of approximately 110 nm, produced during the course of pyrolysis of **1**.

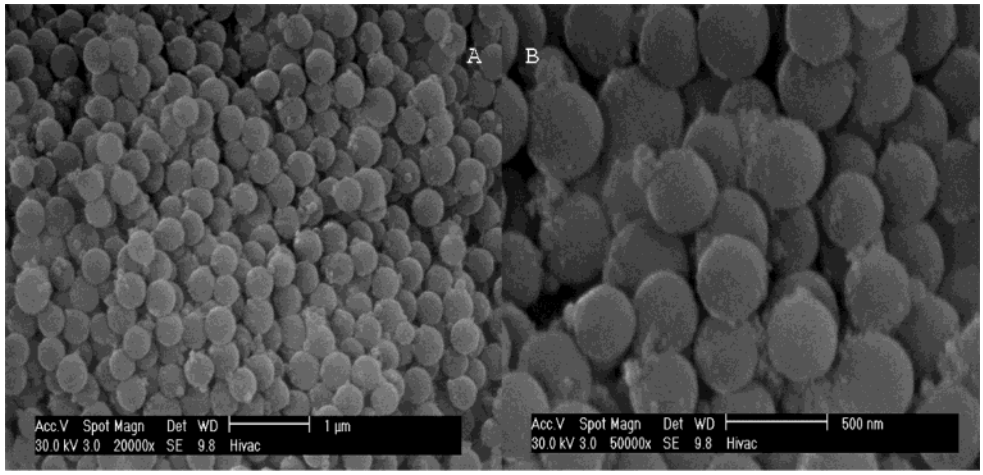

Figure 6. SEM image of oxide spheres produced from the thermal decomposition of **3** at 450 °C for 2 h.

binary oxide systems of bismuth and the later transition metals have not been completely explored and some conflicting reports remain regarding the formation or stable phases of these compositions.

The thermal decomposition of the compounds **2** and **3**, as monitored by TGA/DTA, is very similar to that of **1**. The decomposition of the compounds begins at 190 and 170 °C, respectively, and is complete by 400 °C in both cases. Both compounds exhibit a large exothermic event in the differential thermal analysis that occurs immediately prior to the formation of the final decomposition product; similar to what is observed in **1** and, like **1**, this has been assigned to a reorganization of the oxide lattice as essentially no mass is lost. SEM analysis reveals that **3** decomposes to produce a large number of oxide spheres with an average diameter of 275 nm (Figure 6). The balance of the sample was observed to be amorphous material. Compound **2** was found to behave similarly but produced significantly more amorphous material under identical decomposition conditions and the diameters of the oxide spheres that were produced were found to vary significantly more (175 nm to 1μm) and the particle morphology was less regular. In both cases, the composition of the oxide spheres has been probed by EDX and both metal species were found to be present in the sample.

As noted previously, the ionic conductivity of $Bi_2VO_{5.5}$ is improved by doping the oxide with small amounts of other transition metal species. The phases of oxide produced in this manner are highly sensitive to the amount of dopant included in the reaction mixture.[55] Small amounts of transition metals generally result in the isolation of the high-temperature (γ) phase of $Bi_2VO_{5.5}$, while larger amounts of transition metals tend to result in the formation of the metastable γ' phase of $Bi_2VO_{5.5}$. Both phases of $Bi_2VO_{5.5}$ contain a perovskite structure composed of alternating $(Bi_2O_2)^{2+}$ and $VO_{3.5-x}^{2-}$ layers and are structurally similar to γ-Bi_2MoO_6.[12] The γ phase of $Bi_2VO_{5.5}$ contains significant disorder of both the oxygen vacancies and metallic ion positions. It is this disorder that is responsible for the high ionic conductivity of the material. In converting the sample to the low-temperature α or β phases, there is large-scale ordering of both the oxygen vacancies and of the metal ion positions and the conductivity of the ceramic is effectively quenched.[12] The γ' phase of $Bi_2VO_{5.5}$ is intermediate between the high- and low-temperature forms. This phase does exhibit ordering of the oxygen vacancies and metal ion positions, but still retains

(55) Watanabe, A.; Das, K. *J. Solid State Chem.* **2002**, *163*, 224–230.

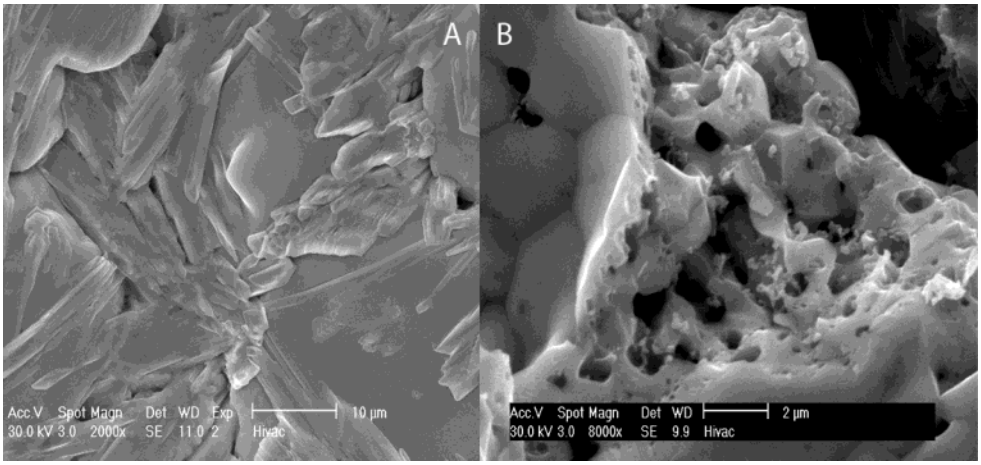

Figure 7. SEM image of the product produced from the pyrolysis of a mixture of **1** and **2** (A) or **1** and **3** (B) for 2 h at 750 °C.

significant conductivity, making it potentially useful for a number of applications. Transition metal dopants are postulated to improve the conductivity of the ceramic by increasing the number of oxygen vacancies in the material,[56] by modulating the ionic potential of the sample,[57] and by preventing the ordering of the oxygen vacancies and metal ion positions.[12,56]

We have investigated whether multimetallic oxides containing bismuth, vanadium, and either copper or nickel are accessible by direct doping of the molecular precursor **1** with samples of **2** or **3** in various ratios prior to thermal decomposition of the samples. A highly crystalline purple material was obtained from the pyrolysis of **2** in the presence of **1** for 2 h at 750 °C. A similar experiment utilizing **3** produced a reddish oxide product. SEM analysis of the products of decomposition reveals that both samples possess well-formed crystallites that are not observed in the thermal decomposition of the molecular precursors alone (Figure 7). The ratio of complexes employed in these experiments was initially intended to approximate the transition metal ratio of the $Bi_2Cu_{0.1}V_{0.9}O_{5.5-\delta}$ systems, although the product material would likely be lean in bismuth due to the stoichiometry of the molecular precursors presented here. In all cases, the product oxide acquired from heating the mixtures at 750 °C for 2 h was found to be composed of a mixture of the anticipated $BiVO_4$ and a transition metal-doped $Bi_2VO_{5.5}$-type phase.

Determination of the fate of the all of the metal species in these experiments is difficult as the powder X-ray diffraction patterns of the termetallic $BiMVO_x$ materials are nearly identical to that of $Bi_2VO_{5.5}$.[55] To investigate more effectively the composition of the oxides produced in this manner, the ratio of the molecular compounds was changed from 10:1 to 1:1. Pyrolysis of this mixture under identical conditions to the initial experiments resulted in the formation of a $Bi_2VO_{5.5}$-type material as the only bismuth-containing phase (Figure 8). Detailed analysis of the complexes produced by doping either **2** or **3** into **1** by both EDX and by powder X-ray diffraction illustrated that the majority of the sample was composed of the γ' phase of $Bi_2V_xM_{1-x}O_{5.5-\delta}$.

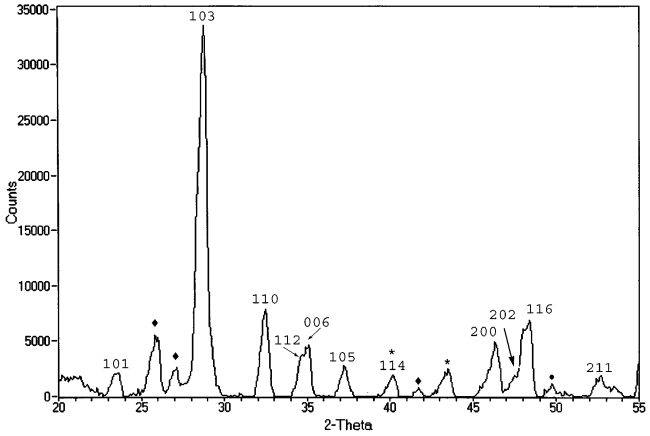

Figure 8. Indexed powder X-ray diffraction spectrum of the thermal decomposition product of a 1:1 mixture of **1** and **3** annealed for 2 h at 750 °C. Peaks are indexed to the γ' phase of $Bi_2V_xM_{1-x}O_{5.5}$. Peaks labeled with an "*" represent NiO, while peaks marked with an "◆" represent an unidentified phase in the material.

Additional byproducts of $Cu_3(VO_4)_2$ (**2**) and NiO (**3**) were also detected in ca. 5% abundance relative to the $Bi_2V_xM_{1-x}O_{5.5-\delta}$ phase in both cases, as indicated by powder X-ray diffraction studies. These byproducts are consistent with the formation of a nonstoichiometric material, and a possible series of reactions leading to the formation of the observed products is provided in eqs 1−3. While the formation of the byproducts observed in this system is not necessarily desirable, similar results are invariably obtained in solid-state syntheses and have not been observed to adversely affect the ionic conductivity of the material.[55]

$$\mathrm{Bi(Hsal)(sal)\cdot V(O)(salen)} \rightarrow \mathrm{BiVO_4} \quad (1)$$

$$\mathrm{Bi(Hsal)_3\cdot Ni(salen)} \rightarrow \mathrm{NiO} + {}^1/_2\mathrm{Bi_2O_3} \quad (2)$$

$$\mathrm{BiVO_4} + {}^1/_2\mathrm{Bi_2O_3} + x\mathrm{NiO} \rightarrow \mathrm{Bi_2V_xNi_{1-x}O_{5.5-\delta}} + x\mathrm{V_2O_5} \quad (3)$$

The formation of a termetallic species as the major product from the doping of **2** or **3** into samples of **1** has also been confirmed by elemental mapping of the bulk oxides (Figure 9). The area that was imaged was large enough so that the signal from the byproduct materials

(56) Simner, S. P.; Suarez-Sandoval, D.; Mackenzie, J. D.; Dunn, B. *J. Am. Ceram. Soc.* **1997**, *80*, 2563−2568.
(57) Sharma, V.; Shukla, A. K.; Gopalakrishnan, J. *Solid State Ionics* **1992**, *58*, 359−362.

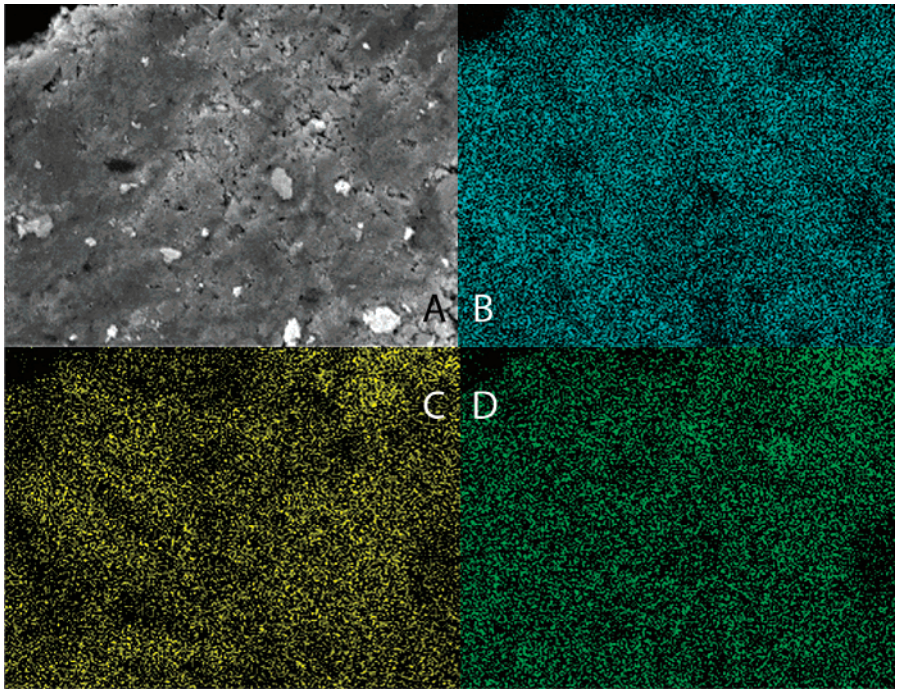

Figure 9. Elemental map detailing homogeneous distribution of the bismuth (B), copper (C), and vanadium (D) in the oxide produced from pyrolysis of a 1:1 mixture of **1** and **2** for 2 h at 750 °C. Section A details the sample that was imaged. The area represented is approximately 200 × 200 μm.

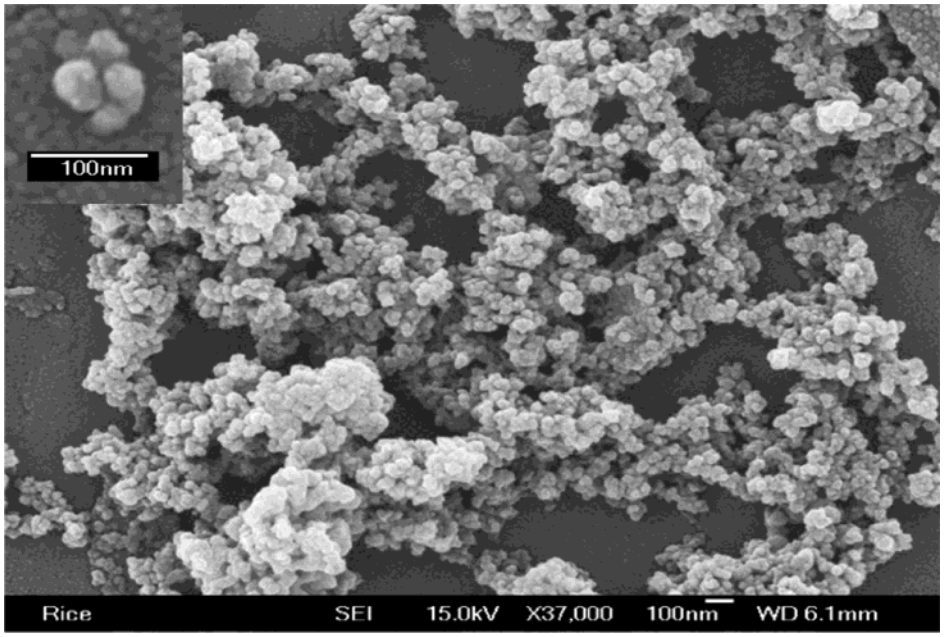

Figure 10. SEM image of the oxide particles produced from the hydrolytic decomposition of **2** in the presence of stearic acid. The dimensions of the particles are on the order of 30−50 nm. The inset image details a cluster of oxide particles produced in this manner.

would not contribute significantly to the total image gathered. The results of the experiments indicate that there is uniform distribution of the three metal species throughout the oxide samples, supporting the formation of the $Bi_2V_{1-x}M_xO_{5.5-\delta}$ phase.

Conclusive determination of the ratios of the transition metals in the samples is complicated by the presence of the byproducts in the oxide mixture; however, it is important to note that previous reports for the synthesis of the γ' phase of $BiMVO_x$ systems via traditional solid-state syntheses reported that conditions of 800 °C for 20 h were required.[55] In contrast, we have been able to synthesize similar complexes at lower temperatures and at significantly reduced reaction periods, clearly illustrating the utility of designed molecular precursors in the synthesis of advanced materials.

Smaller bimetallic nanoparticles have been synthesized by hydrolysis of the molecular precursors in the presence of the stabilizing agents stearic acid and diphenyl ether. The particles that are isolated from this reaction have an average diameter of approximately 40 nm (Figure 10). The materials produced in this manner do not possess the regular spherical morphology typify-

ing the thermal decomposition products; however, these materials were found to be repeatedly dispersible in a variety of solvents. Some aggregation of the particles is observed on isolation of the materials. This has been attributed to loss of the stabilizing diphenyl ether from the surface of the oxide particle. Analysis of the oxides produced using hydrolytic approaches by EDX shows that, similarly to the thermal decomposition methods, the metal stoichiometry of the molecular precursor is conserved in its transformation to the oxide material.

Conclusions

The inherent Lewis acidity of bismuth presents a convenient handle for the synthesis of bimetallic complexes. This approach has been used to successfully synthesize a single-source precursor for the oxide ion-conducting ceramic $BiVO_4$. The bimetallic compounds presented here can be used to synthesize the termetallic system $Bi_2V_{1-x}M_xO_{5.5-\delta}$ (M = Cu, Ni) by simple mixing of the molecular precursors prior to pyrolysis. In all cases, the conditions required for conversion of the molecular precursors to the oxide materials are significantly less than what is required for similar solid-state syntheses.

Acknowledgment. We would like to thank the Robert A. Welch Foundation and the National Science Foundation for support of this work.

Supporting Information Available: Further experimental data relating to the characterization and thermal decomposition of the complexes including mass spectral, TG/DTA, transmission electron and scanning electron micrographs, and EDX spectra have been deposited as Supporting Information (PDF). This material is available free of charge via the Internet at http://pubs.acs.org. Crystallographic data for the complexes discussed in this paper have been deposited at http://pubs.acs.org (CIF) and with the Cambridge Crystallographic Data Center (CCDC). Copies of this information may be obtained free of charge from: The Director, CCDC, 12 Union Road, Cambridge, CB2 1EZ, UK (fax, 44-1233-336-033; e-mail, deposit@ccdc.cam.ac.uk; www: http://www.ccdc.cam.ac.uk).

CM0342851